



Distinct seasonal changes and precession forcing of surface and subsurface temperatures in the mid-latitude North Atlantic during the onset of the Late Pliocene

Xiaolei Pang^{1,2}, Antje H. L. Voelker^{3,4}, Sihua Lu⁵, Xuan Ding⁶

5 ¹Institute of Ocean Research, Peking University, Beijing, 100871, China

²School of Earth and Space Sciences, Peking University, Beijing, 100871, China

³Instituto Português do Mar e da Atmosfera, Divisão de Geologia e Georecursos Marinhos, Av. Doutor Alfredo Magalhães Ramalho 6, 1495-165 Alges, Portugal

10 ⁴Centro de Ciências do Mar do Algarve (CCMAR), Universidade do Algarve, Campus de Gambelas, Edf. 7, 8005-139 Faro, Portugal

⁵State Joint Key Laboratory of Environmental Simulation and Pollution Control, College of Environmental Sciences and Engineering, Peking University, Beijing, 100871, China

⁶School of Ocean Sciences, China University of Geosciences (Beijing), Beijing, 100083, China

Correspondence to: Xiaolei Pang (xiaolei.pang@pku.edu.cn)

15 **Abstract.** The Late Pliocene marks the intensification of Northern Hemisphere Glaciation, offering a unique opportunity to study climate evolution and ice-sheet related feedback mechanisms. In this study, we present high-resolution Mg/Ca-based sea surface (SST) and subsurface temperatures (SubT) derived from foraminiferal species *Globigerinoides ruber* and *Globorotalia hirsuta*, respectively, at the Integrated Ocean Drilling Project (IODP) Expedition 306 Site U1313 in the mid-latitude North Atlantic during the early Late Pliocene, 3.65 – 3.37 million years ago (Ma). We find distinct differences
20 between our new *G. ruber* Mg/Ca-based SST record and previously published alkenone-based SST record from the same location. These discrepancies in both absolute values and variations highlight distinct seasonal influences. The *G. ruber* Mg/Ca-based SST data, reflecting summer temperatures, were primarily influenced by local summer insolation, showing a dominant precession cycle. Conversely, the variations in alkenone-based SST are found to be more indicative of cold season changes, despite previous interpretations of these records as reflecting annual mean temperatures. A simultaneous decline in
25 Mg/Ca-based SST and SubT records from 3.65 to 3.5 Ma suggests a diminished poleward oceanic heat transport, implying a weakening of the North Atlantic Current. A comparison with early Pleistocene *G. ruber* Mg/Ca-based SST records shows a shift in the dominant climatic cycle from precession to obliquity, alongside a marked increase in amplitude, indicating an enhanced influence of obliquity cycles correlated with the expansion of Northern Hemisphere ice sheets.

1 Introduction

30 The Late Pliocene, spanning from 3.6 to 2.58 million years ago (Ma), marks a pivotal transition in Earth's climate history. During this period, the climate shifted from the relatively stable and warm unipolar cool-house climate to the bipolar



glaciated climate states of the ice-house associated with the development of the Northern Hemisphere Glaciation (NHG) (Lisiecki and Raymo, 2005; Westerhold et al., 2020). Marine sedimentary records of oxygen isotopes ($\delta^{18}\text{O}$) reveal that the onset of the NHG (oNHG) can be traced back to as early as ~ 3.6 Ma (Meyers and Hinnov, 2010; Mudelsee and Raymo, 2005). This is followed by an intensification of the NHG (iNHG) at ~ 2.7 Ma, characterized by a significant expansion of ice sheets, as evidenced by the abrupt increase of ice-rafted debris in marine sedimentary records (e.g., Bailey et al., 2013). From the iNHG onwards, the climate dynamics have been characterized by the glacial-interglacial fluctuations of the Northern Hemisphere ice sheets. The presence of ice sheets in the Northern Hemisphere has introduced powerful feedback mechanisms into the Earth's climate system (Meyers and Hinnov, 2010; Westerhold et al., 2020). The Late Pliocene thus provides an unique opportunity to study the characteristics of the climate systems with the involvement of ice-sheet related feedback mechanisms.

The mid- to high-latitude North Atlantic is the region most directly affected by the NHG. The North Atlantic Current (NAC), as the upper limb of the Atlantic Meridional Overturning Circulation (AMOC), currently serves as the primary source of oceanic heat for the high-latitude North Atlantic. It has been hypothesized that changes in the NAC's position or/and intensity may play a crucial role in both the oNHG and iNHG (e.g., Karas et al., 2020; Naafs et al., 2010). Sea surface temperature (SST) has been reconstructed across the northern North Atlantic to evaluate the influence from both the NAC and ice-sheets related feedbacks (Bolton et al., 2018; Karas et al., 2020; Lawrence et al., 2010; Naafs et al., 2020). Previously published Late Pliocene SST records from the mid- to high-latitude North Atlantic suggest warmer-than-present climate, with an overall cooling trend towards the Pleistocene (Naafs et al., 2020; Lawrence et al., 2010). On orbital timescale, SST changes are predominantly influenced by obliquity, with a notable absence of a significant precession cycle (McClymont et al., 2023).

There are a number of studies focusing on the Late Pliocene NAC changes (Karas et al., 2020; Naafs et al., 2010; Friedrich et al., 2013; De Schepper et al., 2009; Bolton et al., 2018; Hennissen et al., 2014). However, contrasting conclusions about NAC changes and its impacts are often drawn when analyzing SST records from various sites and even when examining SST records obtained from different paleotemperature proxies at the same site. For instance, the alkenone-based SST record from the Integrated Ocean Drilling Program (IODP) Site U1313 ($41^{\circ}00'\text{N}$, $32^{\circ}57'\text{W}$) indicates a long-term decreasing trend from 2.9 to 2.5 Ma, with pronounced cooling during glacial periods. Combining alkenone-based productivity records, Naafs et al. (2010) proposed significant weakening of the NAC, especially during severe glacial times. They suggest that during these glacial periods, the NAC's flow direction likely shifted from its current northeastern trajectory to a more west-east direction. This would allow the subarctic front, the boundary between the subtropical (STG) and the subpolar gyre (SPG), to reach the vicinity of Site U1313. Yet, this conclusion is contested by subsequent research at the same Site U1313 (Bolton et al., 2018; Friedrich et al., 2013). Here, higher foraminifera *Globigerinoides ruber* white Mg/Ca-based SST indicate a generally warmer climate during the same time interval, with only modest cooling during glacial periods. This undermines the idea of a substantially weakened NAC and the subarctic front being displaced into the mid-latitudes of Site U1313. Recently, based on a decreasing trend observed in *Globigerina bulloides* Mg/Ca-based SST at Site



610 (53°13'N, 18°53'W) between 3.65 to 3.5 Ma, Karas et al. (2020) proposed that a weakened NAC during this period preconditioned the climate for the oNHG. However, this conclusion is at odds with the warming trend recorded by alkenone-based SST records during the same period from nearby sites (Lawrence et al., 2009; Naafs et al., 2010).

70 The contrasting conclusions about the NAC changes based on the analysis of different SST records, might arise from the use of different proxies that could reflect different seasons. The alkenone-based SST, so far offering the most comprehensive and continuous records in the North Atlantic, are usually interpreted as representing annual mean temperature (Lawrence et al., 2010; Naafs et al., 2010, 2020). However, some studies from the mid-latitude North Atlantic suggest that alkenone-based SST are biased towards recording cold season conditions as a result of spring- or winter-time blooms of coccolithophorids (Bahr et al., 2023; Repschläger et al., 2023).

75 The foraminifera *G. ruber* white and *G. bulloides* are two commonly used species for Mg/Ca-based SST reconstruction in the North Atlantic. The *G. bulloides* Mg/Ca-based SST is usually viewed as reflecting an annual or spring signal (Hennissen et al., 2015; Karas et al., 2020). However, it might lean towards subsurface temperatures due to vertical migrations influenced by factors such as food supply and water column structure (McClymont et al., 2023). Recent research suggests that *G. bulloides* Mg/Ca may represent spring subsurface conditions (Repschläger et al., 2023). On the other hand, 80 for the *G. ruber* white Mg/Ca-based SST, there is a general consensus in literature that it represents summer conditions in the mid-latitude North Atlantic (Bolton et al., 2018; Friedrich et al., 2013; Robinson et al., 2008).

Recent studies have underscored the importance of deep-dwelling foraminiferal species like *Globorotalia inflata* and *Globorotalia crassaformis* in reconstructing subsurface temperatures (SubT) (Bolton et al., 2018; Catunda et al., 2021; Reibsig et al., 2019). Contrary to the marked seasonal variations of SST, especially in mid- and high-latitude regions, SubTs 85 reflect less seasonality. Furthermore, SubT records have demonstrated the capability to identify changes in meridional migration at the gyre boundary, which might not be evident when analyzing SST changes due to surface-related variabilities (Bolton et al., 2018; Catunda et al., 2021; Reibsig et al., 2019).

In this study, we provide high-resolution *G. ruber* white Mg/Ca-based SST and *Globorotalia hirstua* Mg/Ca-based SubT records for the oNHG period (3.65 – 3.37 Ma) at mid-latitude North Atlantic Site U1313 within the STG's northern 90 region (sometimes also referred to as transitional waters; Fig. 1). By combining previously published alkenone-based SST data from the same location, we aim to gain a more detailed view of climate evolution associated with the NAC and the oNHG during the early Late Pliocene. We further compare *G. ruber* Mg/Ca-based SST and alkenone based SST from the early Late Pliocene (3.65 – 3.37 Ma) with those from the Plio-Pleistocene transition (2.8 – 2.4 Ma) at Site U1313. This makes it possible to explore how the amplitude and dominant orbital cycle might have changed over time during the 95 development of the NHG.

2. Material and methods

2.1 Sampling and Age model

IODP Site U1313 (Fig. 1), a re-occupation of Deep Sea Drilling Program (DSDP) Site 607, was retrieved at a water depth of 3426 m from the base of the upper western flank of the Mid-Atlantic Ridge, and four holes were drilled at Site



100 U1313 (Expedition 306 Scientists, 2006). The sediment samples analyzed in this study are from the primary shipboard splice
of holes U1313B and U1313C, spanning the depth interval from 157.21 m to 172.14 m of the adjusted meter composite
depth (amcd) scale (for details on the amcd see (Naafs et al., 2012); U1313B sample retain their original mcd depths). The
10 cc samples were taken over a 2 cm wide sediment interval at a spacing of 5 cm. In total, 323 samples were used for this
study. Epibenthic foraminifera $\delta^{18}\text{O}$ data were obtained for those samples and integrated into the high-resolution benthic
105 foraminiferal $\delta^{18}\text{O}$ record used to generate the age model of Naafs et al. (2020). That age model is based on tuning the
U1313 $\delta^{18}\text{O}$ record to the global LR04 benthic $\delta^{18}\text{O}$ stack (Naafs et al., 2020). Accordingly, the time span corresponding to
the investigated interval is estimated to be 3.65 to 3.37 Ma, with a temporal resolution of approximately 1 thousand years
(kyr) for each sample.

2.2 Foraminiferal species and depth habitats

110 In order to establish temperature records from both surface and subsurface depth, this study utilized two species of
planktonic foraminifera: *G. ruber* (white) and *G. hirsuta*. *G. ruber* white is a mixed layer species with a habitat depth
ranging from 0 to 50 m (Anand et al., 2003), and it is widely used for reconstructing SST across the global ocean. Notably, at
Site U1313, previous studies have indicated that the *G. ruber* white Mg/Ca-based SST represent summer conditions (Bolton
et al., 2018; Friedrich et al., 2013). On the other hand, *G. hirsuta* is a deep thermocline species with a habitat depth ranging
115 from 0 to 800 m within the North Atlantic (Cléroux et al., 2013), but maximum abundances between 300 and 500 m in the
vicinity of the Azores Islands (Rebotim et al., 2019). Its depth range, therefore, overlaps with *Globorotalia crassaformis*,
which was used for reconstructing SubT at Site U1313 in the early Pleistocene (Catunda et al., 2021; Bolton et al., 2018). *G.*
hirsuta was chosen to reconstruct SubT due to its abundance and *G. crassaformis* not being consistently observed within our
study interval.

120 2.3 Mg/Ca analysis and Paleotemperature reconstruction

The specimens for the trace element analyses were collected from the residue $>63\ \mu\text{m}$ of the sediment samples
treated in the Sedimentology and Micropaleontology laboratory of LNEG (now integrated into the Marine Geology Division
of IPMA) for the stable isotope analyses. After weighing and freeze drying, the sediment samples were washed through a 63
 μm mesh sieve, the sand sized residue dried on filter paper at 40°C and then weighted. For the trace element analyses,
125 approximately 30 individual tests of *G. ruber* white and 20 of *G. hirsuta* were selected from the size fraction of 250 to 355
 μm . The foraminiferal tests were gently crushed between two glass plates under a binocular microscope. The resulting
crushed samples were subsequently transferred to 500 μl centrifuge tubes for further cleaning. The cleaning procedure
adhered to the methods outlined in Barker et al. (2003) without using the reductive step. After cleaning, each sample was
dissolved within a 0.075M HNO_3 solution followed by centrifugation to eliminate any residual particulate impurities. The
130 resulting supernatant solution was transferred to a new 500 μl centrifuge tube. Measurements of Mg, Ca, Al, and Mn
concentrations were carried out using inductively coupled plasma mass spectrometry (ICP-MS, Bruker aurora M90) at
Peking University. Al/Ca and Mn/Ca ratios were used for examining the cleaning efficiency. The Al values are usually lower
than the detection limit of the ICP-MS. No anomalous Mg/Ca ratios were observed, nor was there any relationship between



Mg/Ca and Mn/Ca ratios (Supplementary Fig. S1 and S2). Thus no Mg/Ca data were rejected. The long-term reproducibility
135 of Mg/Ca measurements, obtained by replicating analyses of a standard solution along with samples over a four-month
testing period, is $\pm 0.4\%$ (1σ).

The residence time for Ca and Mg in the ocean are approximately 1 and 13 million years (Myr), respectively. Over
the Cenozoic, the Mg/Ca ratio of seawater (Mg/Ca_{sw}) has exhibited notable secular variations (Zhou et al., 2021). Therefore,
when using foraminiferal Mg/Ca ratios for reconstructing ocean temperatures for time periods exceeding 1 Myr, one needs to
140 account for the influence of Mg/Ca_{sw} variations (Evans and Müller, 2012). In order to address this concern, the measured
Mg/Ca (Mg/Ca_{meas}) are corrected for the change in Mg/Ca_{sw} (Zhou et al., 2021) by using the following relationship from
Evans and Müller (2012): $Mg/Ca_{corr} = Mg/Ca_{meas} * \{(5.3/(Mg/Ca_{sw})\}^H$. The power coefficient H was set to 0.4 following the
recommendation in the paper (Evans and Müller, 2012). It is worth noting that, considering that the duration of our study
interval is less than 1 Myr, the applied correction does not induce alterations to trends or the relative temperature variations
145 (Supplementary Fig. S3).

The corrected Mg/Ca ratios were converted to temperatures using the formula of $Mg/Ca = 0.38 \pm 0.02 \exp$
($0.09 \pm 0.003 * T$) for *G. ruber* white (Anand et al., 2003) and the species-specific calibration $Mg/Ca = 0.2 \pm 0.07 \exp$
($0.18 \pm 0.057 T$) for *G. hirsuta* (Cléroux et al., 2013). The total uncertainties in reconstructed temperatures were estimated by
propagating the uncertainties introduced by Mg/Ca measurements and temperature calibrations. The total uncertainties are
150 on average about ± 1 °C (1σ) for *G. ruber* Mg/Ca-based SST and ± 4.7 °C (1σ) for *G. hirsuta* Mg/Ca-based SubT. The
considerable uncertainty associated with *G. hirsuta* Mg/Ca-based SubT arises from the significant uncertainty in its
calibration. However, since we do not use the SubT data to compare with other proxy records or for calculating other
products, this uncertainty does not impact our study.

2.4 Spectral analysis

155 Spectral analysis was conducted by using the REDFIT module from the PAST4 software package (Hammer and
Harper, 2001), the settings for the analysis are the same for all the records: Window = Welch, Oversampling = 3 and
Segments = 3. For the purpose of filtering the data, the software package AnalySeries 2.0 was utilized (Paillard et al., 1996).

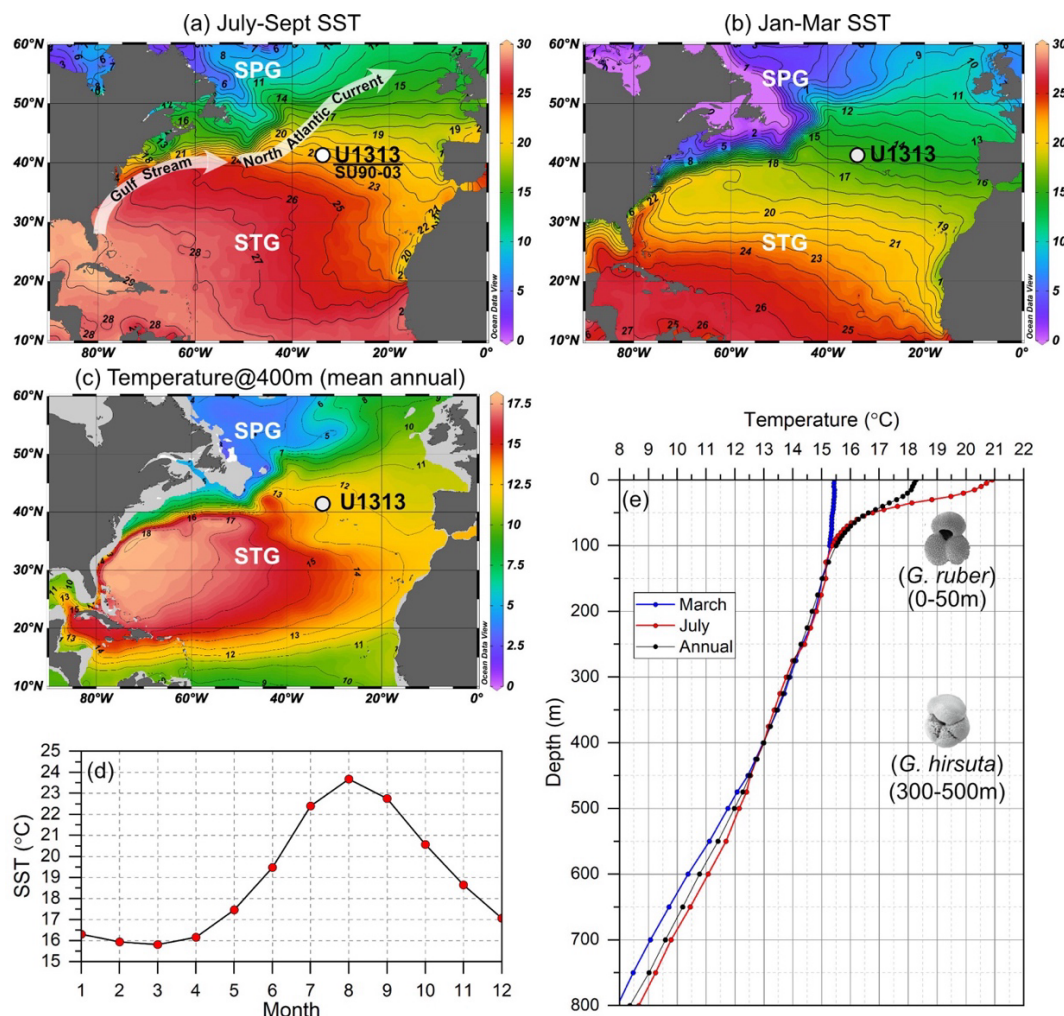


Figure 1. The location of Site U133 and modern oceanographic settings. (a) Summer season (July to September) mean surface temperature. the main route of warm current Gulf Stream and its northern extension, the North Atlantic Current, are also presented. STG is subtropical gyre, SPG is subpolar gyre. Site SU90-03 which provides core top Mg/Ca ratios is presented by the same point of U133 due to the proximity of locations. The actual sites are distinct but are located very close to each other. (b) Winter season (January to March) mean surface temperature and (c) mean annual water temperature at depth of 400 m. (d) Modern monthly mean surface temperature at site U133, averaged from 2000 – 2015 derived from the Simple Ocean Data Assimilation (SODA) database (Carton and Giese, 2008). (e) Depth profile of temperature during different seasons at site U133, and the two studied planktonic foraminiferal species with their habitat depth indicated. Temperature data in (a), (b), (c) and (e) are sourced from the World Ocean Atlas 2013 (Locarnini et al., 2013).

3. Results

3.1 Mg/Ca and Temperature

The Mg/Ca ratios and resulting SST obtained for the *G. ruber* samples exhibit a range of 2.9 to 3.9 mmol/mol and 23.2 to 26.6 °C, respectively (Fig. 2). The SST record exhibits small-scale oscillations over the course of the period. The



highest value is observed at ~3.61 Ma, while the lowest value is approximately around 3.47 Ma. A distinct declining pattern is evident between 3.65 and 3.47 Ma.

As for the Mg/Ca ratios and the estimated SubT temperatures derived from the *G. hirsuta* samples, the values fluctuate within the range of 1.9 to 2.5 mmol/mol and 11.7 to 13.2 °C, respectively. Notably, two distinct decreasing trends are observed in the SubT record. The first trend, similar to the SST record, spans from 3.65 to 3.5 Ma, while the second trend commences from 3.45 Ma onwards.

3.2 Spectral analysis results

Spectral analysis results for both *G. ruber* white Mg/Ca-based SST and *G. hirsuta* Mg/Ca-based SubT records from this study indicate prominent peaks at frequencies corresponding to the precession (19 – 23 kyr) and obliquity cycles (41kyr) (Fig. 3). The precession cycle is the predominant influence on the *G. ruber* white Mg/Ca-based SST, while the *G. hirsuta* Mg/Ca-based SubT is primarily governed by the obliquity cycle. Although the 100-kyr cycle appears in the spectral analysis results, it is not reliable as the short time span of the dataset (~ 300 kyr) does not allow for a statistically sound interpretation.

For further comparison, spectral analysis were also conducted on previously published alkenone-based SST records from the two intervals of 3.7 – 3.3 Ma and 2.8 – 2.4 Ma and on the *G. ruber* white Mg/Ca-based SST record from the younger period (2.8 – 2.4 Ma) at Site U1313. The results indicate that these records are all dominated by obliquity, with a notable absence of a significant precession cycle.

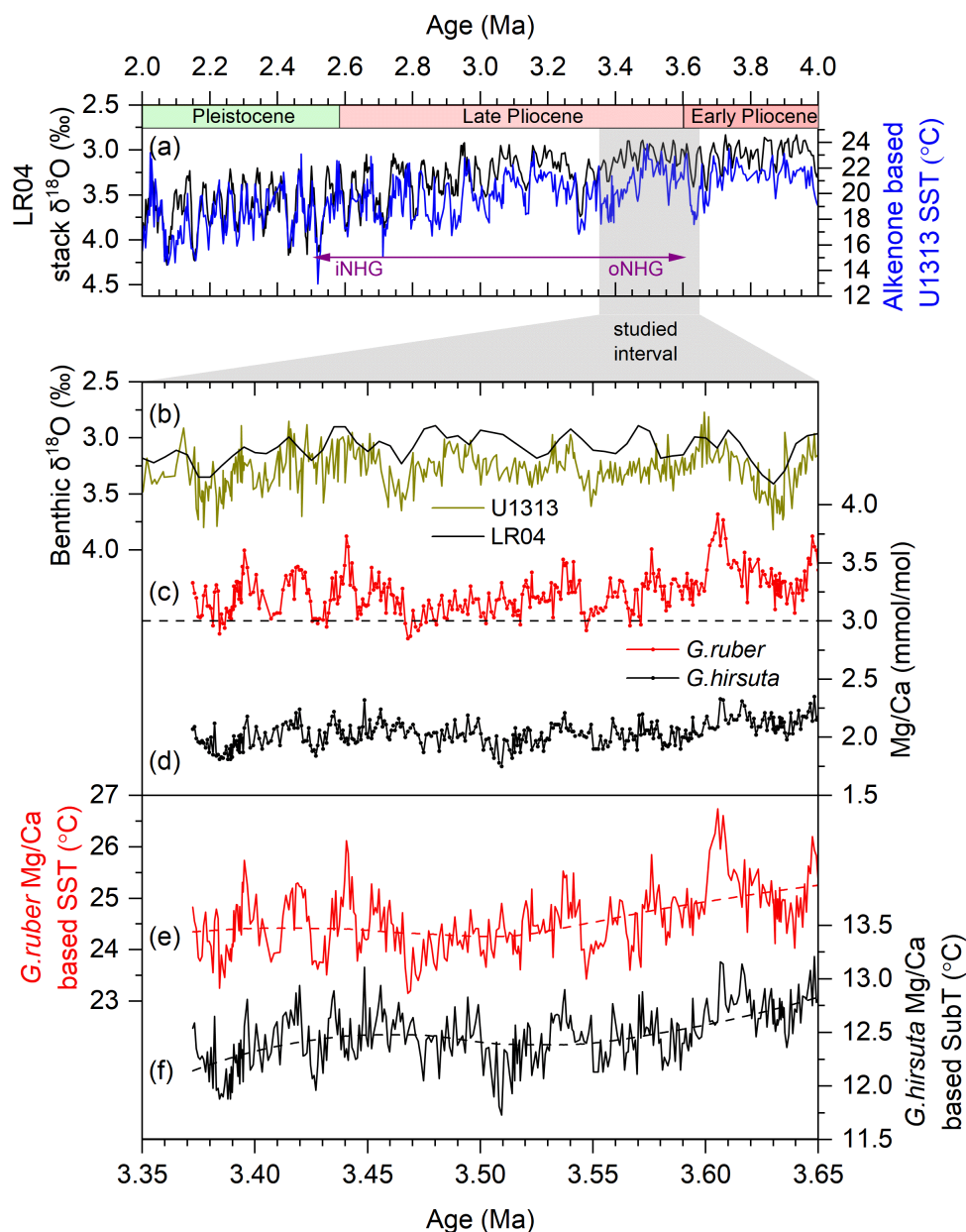
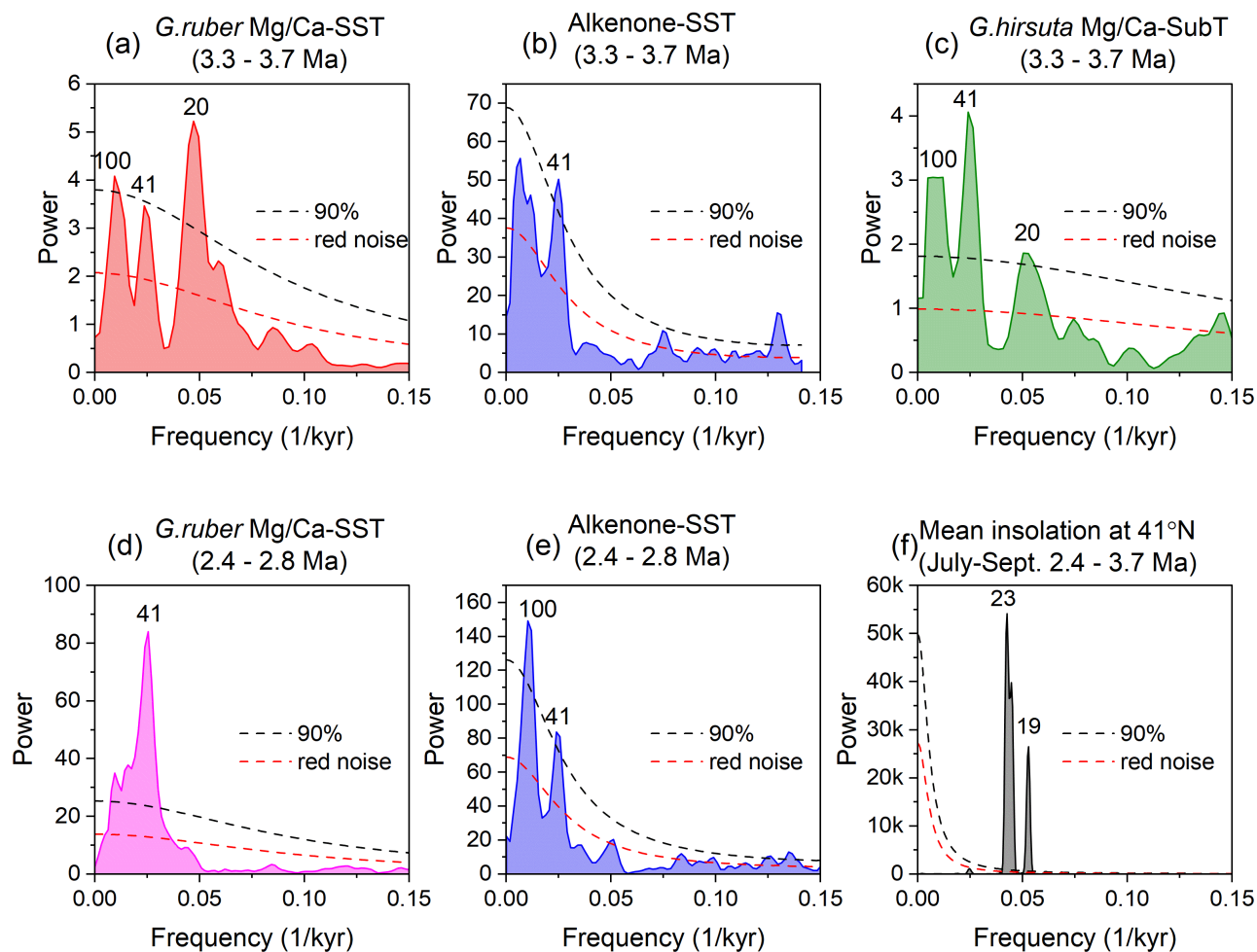


Figure 2. The studied interval and paleoclimate data reconstructed from Site U1313. (a) The LR04 global benthic $\delta^{18}\text{O}$ stack (Lisiecki and Raymo, 2005) and alkenone-based SST from Site U1313 (Naafs et al., 2020), the studied interval (3.65 – 3.35 Ma) is marked by the grey bar. (b) The LR04 benthic $\delta^{18}\text{O}$ stack and benthic $\delta^{18}\text{O}$ record from Site U1313, which has 0.64 per mil added to the original *Cibicidoides* sp. values (Naafs et al., 2020). (c) *G. ruber* Mg/Ca record, with the dashed line indicating the core top *G. ruber* white Mg/Ca value of 3 mmol/mol at site SU90-03. (d) *G. hirsuta* Mg/Ca record. (e) *G. ruber* white Mg/Ca-based SST record and (f) *G. hirsuta* Mg/Ca-based SubT record. Dashed line in (e) and (f) indicates smoothed curve by using Locally Estimated Scatterplot Smoothing (LOESS) to reveal underlying long-term trends.

190



195

Figure 3. Spectral analysis results of paleoclimate records from Site U1313. *G. ruber* white Mg/Ca-based SST and *G. hirsuta* Mg/Ca-based SubT records in (a) and (c) are from this study. Alkenone-based SST records in (b) and (e) from Naafs et al. (2020). *G. ruber* white Mg/Ca-based SST records in (d) from Bolton et al. (2018) and Friedrich et al. (2013). (f) Mean insolation records are obtained from (Laskar et al., 2004). For details on the spectral analyses settings see subchapter 2.4.

200

4. Discussion

Our high-resolution Mg/Ca-based SST and SubT records provide new insights into climate dynamics of the mid-latitude North Atlantic during the early Late Pliocene, a period that marks the oNHG. The Mg/Ca-based SSTs exhibit distinct variations in both long-term trends and dominant orbital cycles compared to the previously published alkenone-based SST (Fig. 4), implying varying seasonal sensitivity of these proxies and thus seasonal SST changes in the mid-latitude North Atlantic in the early Late Pliocene. Our Mg/Ca-based SST and SubT records exhibit a simultaneous cooling trend from 3.65 to 3.5 Ma, contrasting with the warming trend observed in the alkenone-based SST records from the same period, providing an alternate view on the meridional heat transport and associated NAC variations. On orbital timescales, we

205



observed a variety of dominant orbital cycles among Mg/Ca-based SST, SubT, and alkenone-based SST, indicating they are influenced by distinct mechanisms. Below, we focus on these critical features and discuss the driving forces behind them.

210 4.1 The warmth of mid-latitude North Atlantic in early Late Pliocene

The Late Pliocene is known for its global warmth, and is particularly pronounced in mid- to high-latitudes (Fedorov et al., 2013; McClymont et al., 2023). Previously reconstructed SST records spanning the study interval (3.65 – 3.35 Ma) in the mid- to high-latitude North Atlantic consistently indicate warmer-than-present temperatures (Karas et al., 2020; Lawrence et al., 2009; Naafs et al., 2010). Our new Mg/Ca-based SST confirms this Late Pliocene warmth.

215 The Mg/Ca-based SST consistently exceed the modern summer average of 23 °C (July-September, averaged from 2000-2015) at Site U1313 (Fig. 4), suggesting a warmer-than-present mid-latitude North Atlantic in early Late Pliocene. To avoid the potential biases from the selection of Mg/Ca calibration and from the procedure of seawater Mg/Ca correction for this result, we further compared our *G. ruber* white Mg/Ca ratios with that of a core top sample from nearby core SU90-03 (40°30'N, 32°W; Fig. 1a, represented by same dot as U1313). The core top sample of SU90-03, estimated from the period of
220 0 – 4 ka, was non-reductively cleaned (the same method as used in this study) (Cléroux et al., 2008), thus no methodological bias occurs. Our *G. ruber* Mg/Ca ratios, whether or not adjusted for the secular variations of the seawater Mg/Ca, are generally above the value of 3 mmol/mol noted in the core top sample (Fig. 2c and Supplementary Fig. S3). Converting this core top *G. ruber* Mg/Ca ratio to temperature using the calibration selected in this study yields ~ 23 °C, which matches the modern summer temperature in this region. This supports the reliability of the selected calibration of Mg/Ca thermometry
225 and reinforces the finding of the warmer-than-present summer SST at Site U1313 during the Late Pliocene.

What mechanism maintains the warmer SST at Site U1313 during the early Late Pliocene? The northward expansion of the STG's warm waters is likely the most important factor. The Pliocene is characterized by the substantial reduced meridional temperature gradient as clearly evidenced for the mid-Piacenzian Warm Period (Dowsett et al., 2012, 2016; Haywood et al., 2016). In the North Atlantic, the SST gradient from the equatorial to mid-latitude regions was up to
230 5°C smaller during the Pliocene compared to the Pleistocene (Fedorov et al., 2013; Dowsett et al., 2012), whereby the Pliocene SST increase is particularly pronounced in the mid- to high-latitudes (Fedorov et al., 2013; McClymont et al., 2023). The role of atmospheric CO₂ on the warmer climate remains uncertain due to the sparse paleo-CO₂ records available for the whole Pliocene and their significant uncertainties. Recently, the International Consortium of Cenozoic CO₂ Proxy Integration Project (CenCO2PIP) has vetted and synthesized the reliable paleo-CO₂ data available over the past 66 million
235 years (CenCO2PIP Consortium et al., 2023). We incorporated their paleo-CO₂ data for our study interval in Fig. 4c. The CO₂ concentration averaged around 300 ppm with a maximum value generally not exceeding 360 ppm, as recorded in the year 2000, and is in the same range as the high-resolution reconstruction for 3.35-3.15 Ma, i.e. immediately following our study period (de la Vega et al., 2020). Considering the reconstructed SSTs are warmer than the average temperature from 2000 to 2015 (Fig. 1d), the relatively higher CO₂ could not be the primary cause of the warmer temperature during the late Pliocene.
240 Fedorov et al. (2013) have demonstrated that CO₂ is not necessary for the warmer Pliocene climate. Therefore, we attribute



the higher SST observed at Site U1313 during the early Late Pliocene primarily to the northward expansion of the North Atlantic's STG.

4.2 Distinct seasonal variations of SST during the early Late Pliocene: Comparing Mg/Ca- and alkenone-based SST

Compared to the previously published alkenone-based SST from the same location, our new *G. ruber* white Mg/Ca-
245 based SST record provides a different picture on the climate dynamics in the mid-latitude North Atlantic during the Late Pliocene. The *G. ruber* white Mg/Ca-based SST significantly differs from the alkenone-based SST in terms of both absolute values and changing patterns (Fig. 4c,d).

The Mg/Ca-based SST are overall higher than the alkenone-based SST, a pattern in line with previous observations at Site U1313 (Friedrich et al., 2013; Robinson et al., 2008). This difference can be attributed to the fact that *G. ruber* white
250 Mg/Ca-based temperature reflects summer conditions (Repschläger et al., 2023; Robinson et al., 2008), whereas alkenone temperature represents annual mean or spring conditions (Naafs et al., 2020; Repschläger et al., 2023).

However, contrary to previous findings for the early Pleistocene that *G. ruber* white Mg/Ca and alkenone-based SST show generally synchronized variations (Bolton et al., 2018; Friedrich et al., 2013), our *G. ruber* white Mg/Ca-based SSTs display markedly different patterns in both the long-term trends and the dominant orbital cycles (Fig. 4c,d). The
255 Mg/Ca-based SST shows a declining trend from 3.65 to 3.5 Ma, while the alkenone-based SST increases during the same period. Subsequent to 3.5 Ma, the alkenone-based SST notably decreases, while the Mg/Ca-based SST remains relatively stable.

A recent study from the vicinity of the Azores Islands to the south of Site U1313 suggests that the alkenone-based SST predominantly records spring temperatures (Repschläger et al., 2023). The alkenones are produced by coccolithophores
260 that proliferate during spring blooms (March to May) in the mid-latitude North Atlantic (Cavaleiro et al., 2018; Lévy et al., 2005). As illustrated in Fig. 1d, March and April still fall within the coldest SST range at Site U1313. Although it is not certain that alkenone-based SSTs exclusively represent spring temperature in our study interval, it can be reasonably concluded that they are biased towards recording cold season temperature variations.

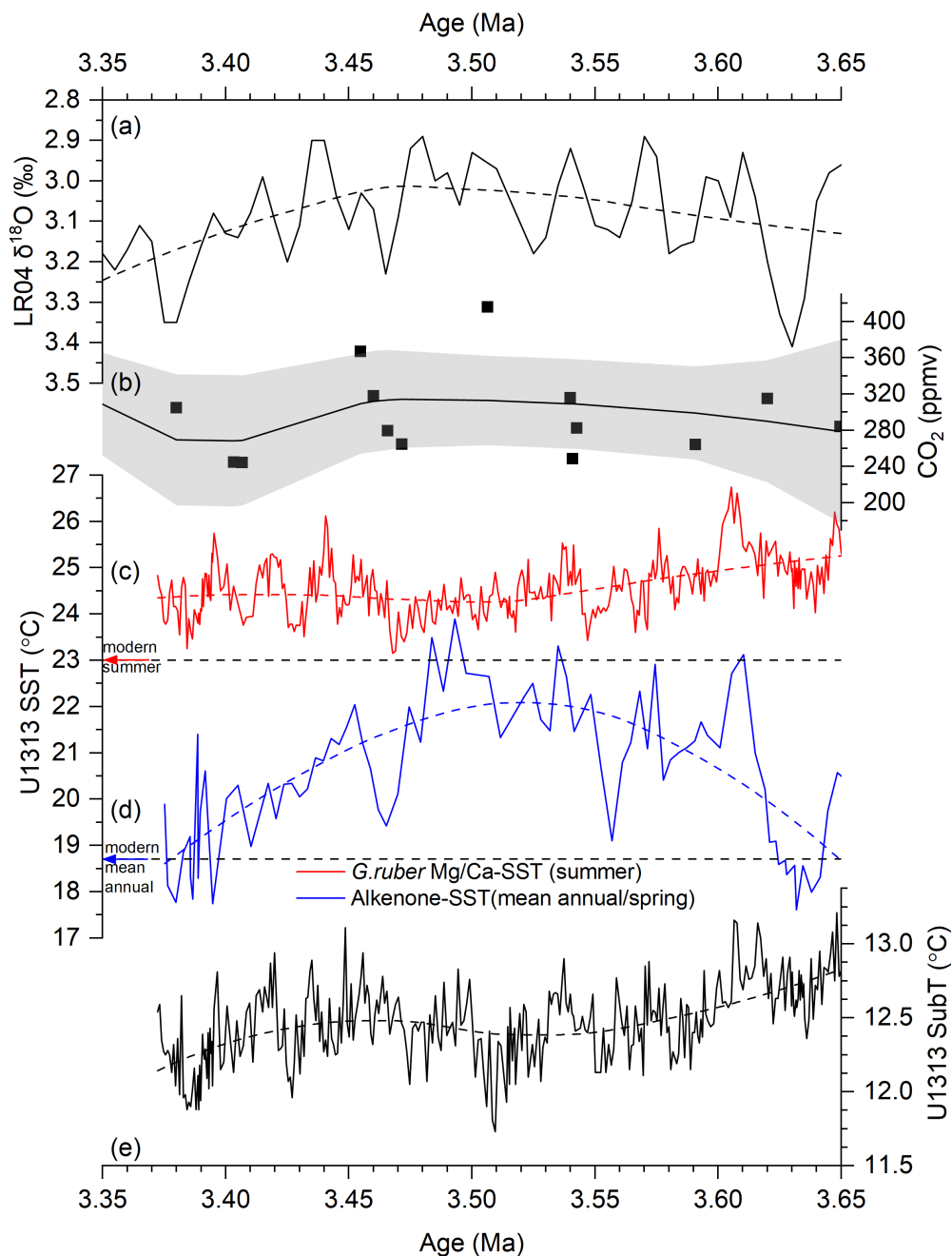
Therefore, the distinct changing patterns of Mg/Ca- and alkenone-based SST records at Site U1313 indicate that
265 during the early Late Pliocene warm and cold season SST variations were influenced by different processes. The *G. ruber* white Mg/Ca-based SST is dominantly controlled by precession and shows a high correlation with local summer insolation (Fig. 5b). Presently located near the northern edge of the STG, the warmer-than-present *G. ruber* white Mg/Ca-based SSTs during the early Late Pliocene imply that Site U1313 was consistently under the influence of the STG's warmer waters during the summer season. We propose that summer insolation forcing and associated STG variations are the primary drivers
270 shaping the warm season *G. ruber* white Mg/Ca-based SST variations at Site U1313.

In contrast, the alkenone-based SSTs, dominated by obliquity and with no sign of precession's influence (Fig. 3b), varied in phase with the benthic foraminiferal $\delta^{18}\text{O}$ record (Fig. 5c), indicating a strong correlation between cold season SST and ice sheet-related feedbacks. Obliquity, while having negligible effects on local insolation variations, plays a critical role in influencing the meridional thermal gradient. The ice-related albedo feedback tends to amplify the obliquity-induced



275 thermal gradient. Changes in the meridional thermal gradient significantly affect the position and strength of the westerlies
over the study region (Bridges et al., 2023; Naafs et al., 2012). These westerlies can impact surface temperatures by inducing
excessive heat loss from the air-sea interface and by influencing the mixing of upper waters (Fan et al., 2023). During the
oNHG, despite the absence of large-scale ice sheets, the seasonal presence of sea ice and the extent of thin ice sheets might
have been significant (Clotten et al., 2018; Knies et al., 2014). Additionally, the reduction or disappearance of sea ice and the
280 thin ice sheets during the warm season could explain why this high-latitude feedback does not dominate the Mg/Ca-based
summer SST. Lawrence et al. (2009) proposed a similar mechanism to explain the unexpectedly high amplitude of alkenone-
based SST observed in the high-latitude North Atlantic during the early Pliocene warm period.

Inconsistencies between foraminiferal Mg/Ca- and alkenone-based SSTs are frequently observed and are mainly
attributed to the different seasons and water depths they represent (Lawrence and Woodard, 2017; Leduc et al., 2010).
285 Moreover, the specific seasons and depths indicated by each proxy may vary across time and location (Leduc et al., 2010). In
many cases from the Pleistocene, both proxy records exhibit similar variations on the glacial-interglacial timescale, and
occasionally, they present similar values (Lawrence and Woodard, 2017; Lee et al., 2021). This means that these two proxies
can be used interchangeably for estimating climate changes under certain conditions (Lawrence and Woodard, 2017).
However, in our case, the SST records provided by the two proxies are different in both variations and values, which means
290 they cannot be used interchangeably. We attribute these discrepancies in our study interval to the distinct seasonal variations
at our site in the early Late Pliocene, a period when the Northern Hemisphere ice sheet related feedback was not strong
enough to synchronize changes in SSTs of both warm and cold seasons. This highlights the importance of employing a
multi-proxy approach to fully understand the characteristics of the climate system.



295 **Figure 4.** Distinct seasonal changes of SST records at Site U1313 during the early Late Pliocene. (a) The LR04 global benthic $\delta^{18}\text{O}$ stack (Lisiecki and Raymo, 2005). (b) Paleo- CO_2 data available during the study interval (CenCO2PIP Consortium et al., 2023), with the black line indicating the smoothed curve with 95% confidence interval. (c) *G. ruber* white Mg/Ca-based summer SST. (d) Alkenone-based SST (Naafs et al., 2020). (e) *G. hirsuta* Mg/Ca-based SubT. Dashed lines in (a), (c), (d) and (e) indicate smoothed curve by using Locally Estimated Scatterplot Smoothing (LOESS) to reveal underlying long-term trends.



300 4.3 North Atlantic Current changes in the early Late Pliocene

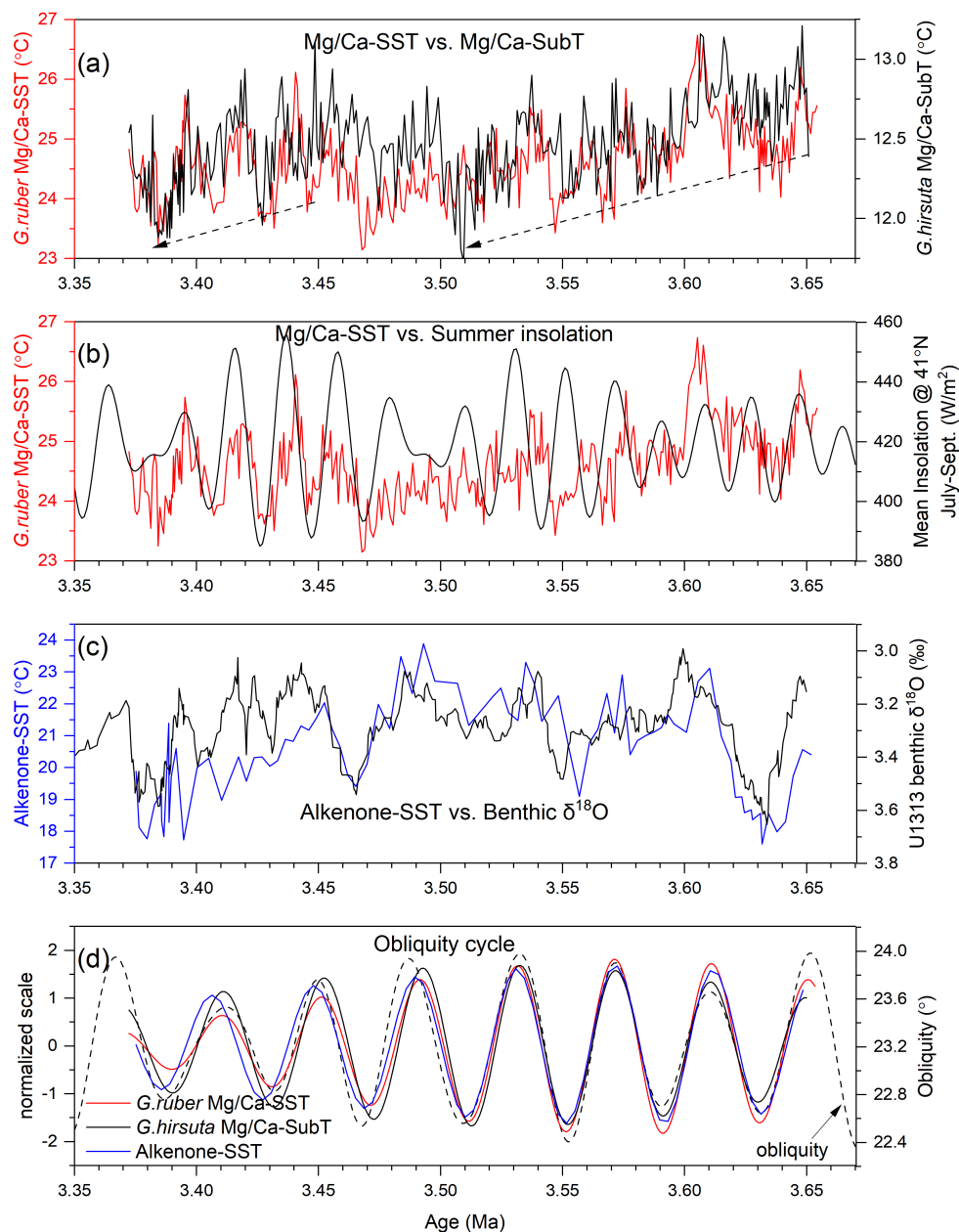
The variations in poleward heat transport associated with the NAC has been considered important in influencing climate variations in the mid- to high-latitude North Atlantic, as well as in the evolution of the NHG (Karas et al., 2020; Naafs et al., 2010). Changes in SST records reconstructed from this region have commonly been linked to NAC variations (Bolton et al., 2018; Lawrence et al., 2009; Naafs et al., 2010). At our study location, Site U1313, situated near the modern
305 northern boundary of the STG, the SST was considered particularly sensitive to northward heat transport and NAC variations (Bolton et al., 2018; Friedrich et al., 2013; Naafs et al., 2010).

The warmer-than-present SST observed at Site U1313 suggests a persistent northward extension of the STG during our study interval. This implies that the NAC maintained an overall high intensity during this period. Within this context, both Mg/Ca- and alkenone-based SST records show long-term trends, implying changes in the meridional heat transport.
310 However, the contrasting trends observed between the Mg/Ca- and alkenone-based SST complicate a straightforward interpretation of NAC variations.

Our new *G. hirsuta* Mg/Ca-based SubT records provide new evidence on the changes in the meridional oceanic heat transport. Unlike the significant seasonal fluctuations observed at the surface, the subsurface waters inhabited by *G. hirsuta* (300 – 500m) display minimal seasonality (Fig. 1e). This reduced seasonality provides a clearer signal of long-term trends,
315 which is free from the noise of seasonal variations. As shown in Fig. 4e, the Mg/Ca-based SubT exhibits a small but significant two-step cooling, each corresponding to the Mg/Ca- or alkenone-based SST records.

During the period between 3.65 and 3.5 Ma, the Mg/Ca-based SubT exhibited a cooling of about 1°C, implying a contraction of the STG. Concurrently, the Mg/Ca-based summer SST showed a corresponding decrease of around 1.5°C (Fig. 4c and Fig. 5a). This consistent cooling trend in both surface and subsurface water depths provides strong evidence for
320 the decrease in northward heat transport, implying the weakening of the NAC. This aligns with findings from a recent study which suggests a weakened NAC in response to a weaker AMOC strength during the same period (Karas et al., 2020). In contrast, the alkenone-based SST shows an approximate 4°C increase, implying that the cold season SST variations was not directly connected to NAC changes. The alkenone-based SST appears to follow changes in benthic $\delta^{18}\text{O}$ (Fig. 5c), suggesting that the cold season trend could stem from alterations from Northern Hemisphere ice coverage.

From 3.45 Ma onwards, the Mg/Ca-based SubT exhibits a second step of cooling, but with a smaller temperature change (~ 0.5°C), suggesting a modest contraction of the STG. The alkenone-based SST shows a clear decreasing trend (~ 4°C), but with an earlier onset at around 3.5 Ma (Fig. 4d), which has been previously explained as a result of a weakened NAC by Naafs et al. (2010). However, the absence of a corresponding clear trend in the Mg/Ca-based SST records suggests that any changes in the NAC were too minor to impact the summer SST significantly. This implies that the 4°C decrease
330 observed in the alkenone-based cold season SST cannot be entirely attributed to NAC changes. Additionally, a clear decreasing trend in the benthic $\delta^{18}\text{O}$ record indicates an increase in ice coverage in the Northern Hemisphere. We propose that the primary driver behind the significant decrease in alkenone-based SST is associated with the ice-related albedo feedback rather than changes in the NAC.



335 **Figure 5.** Comparison of *G. ruber* white Mg/Ca-based SST and *G. hirsuta* Mg/Ca-based SubT. (a) *G. ruber* white Mg/Ca-based SST (red)
 and *G. hirsuta* Mg/Ca-based SubT (black) records, with dashed arrows indicating long-term trends. (b) The comparison between *G. ruber*
 white Mg/Ca-based SST and mean insolation of July to September at 41°N (Laskar et al., 2004). (c) Comparison between the LR04
 benthic δ¹⁸O stack (Lisiecki and Raymo, 2005) and the alkenone-based SST (Naafs et al., 2010). (d) Comparison between obliquity and
 filtered Mg/Ca-based SST, SubT and alkenone-based SST. Gaussian filtering, done with the software AnalySeries 2.0 (Paillard et al.,
 340 1996), centered at the frequency of 0.025 ± 0.003 , i.e., the obliquity band.



4.4 From Precession to Obliquity: The Shifting Dominance in Late Pliocene – Early Pleistocene Sea Surface Temperature in the mid-latitude North Atlantic

By combining the previously published *G. ruber* white Mg/Ca- and alkenone-based SST data from the latest Pliocene and early Pleistocene with the new Mg/Ca records from this study during the early stage of the Late Pliocene, makes it possible to explore the changes in amplitude and pacing of climate change in mid-latitude subtropical North Atlantic during the NHG.

In the Plio-/Pleistocene transition interval of 2.8 – 2.4 Ma, the *G. ruber* white Mg/Ca ratios were sourced from the study of Bolton et al. (2018) and Friedrich et al. (2013). Initially, the Mg/Ca ratios were corrected for changes in seawater Mg/Ca and subsequently converted to temperature using the same methodology and calibration as outlined in the present study. Notably, for the time period of 2.8 – 2.4 Ma, the selected *G. ruber* white specimens belong to the *sensu stricto* morphotype (212-250 μm) with a narrower calcification depth of 0-30 m (Bolton et al., 2018; Friedrich et al., 2013). In comparison, the *G. ruber* white specimens selected for this study include both the *sensu stricto* and the *sensu lato* morphotypes (250 – 350 μm), inhabiting a broader calcification depth of 0 – 50 m (Anand et al., 2003). A Previous study revealed a decrease in Mg/Ca with increasing test size for the species *G. ruber* white (Friedrich et al., 2012). Therefore, the utilization of the smaller sized *G. ruber* (s.s.) with a narrower calcification depth during the 2.8-2.4 Ma interval is likely responsible for the slightly higher interglacial SST values inferred during the early Pleistocene in comparison to those of the supposedly warmer Late Pliocene (Fig. 6b). However, such difference in specimen size and calcification depths are not anticipated to notably affect the relative trends and periodicity of Mg/Ca-based temperatures.

When comparing the *G. ruber* white Mg/Ca-based SST records for our study interval and the Plio-/Pleistocene transition, two significant differences in terms of amplitude and periodicity emerge (Fig. 6). First, the amplitude of SST variations increases from approximately ~ 2 °C during the Late Pliocene to ~ 4 °C in the early Pleistocene. Second, there is a transition in the dominant cycle from precession to obliquity, with the precession cycle being absent between 2.8 – 2.4 Ma (Fig. 3d). Such a transition is not evident in the alkenone-based SST record (Fig. 3b,e).

During the early Late Pliocene (3.65 – 3.37 Ma), obliquity is the dominant cycle in both the alkenone-based SST and the *G. hirsuta* Mg/Ca-based SST records, while being a secondary component in the *G. ruber* Mg/Ca-based SST records (Fig. 3). When filtering the three SST records for the obliquity band, synchronous variations are observed (Fig. 5d), suggesting a common process. As previously discussed in section 4.2, we suggest that the obliquity-induced thermal gradient and associated changes in the westerlies are the primary processes at play. During the oNHG, the seasonal ice coverage were significant to effect cold season SST, but it did not persist through the summer. This resulted in precession remaining the dominant cycle in the summer SST records.

During the 2.8 – 2.4 Ma interval, changes in both Mg/Ca- and alkenone-based SST records were aligned with the benthic $\delta^{18}\text{O}$ record, indicating a dominant obliquity cycle and the absence of the precession cycle. Starting from the iNHG, ice sheets experienced significant growth during glacial periods compared to those of the early Late Pliocene, maintaining substantial volume even in summer. The expansion of the ice sheets amplified the ice-related albedo effect and the influence



375 of obliquity. A noticeable glacial southward shift and intensification of the westerlies occurred after 2.7 Ma (Naafs et al.,
 2012), and from 2.6 Ma southward reflection of the subarctic (subpolar) front occurred (Bolton et al., 2018; Hennissen et al.,
 2014). These processes contributed to lower temperatures at Site U1313 during glacial periods (Bolton et al., 2018; Naafs et
 al., 2012). As a consequence, the increased amplitude of temperature variations associated with the obliquity cycle
 380 overshadowed those of the precession cycle, causing the precession cycle to vanish from spectral analysis results. Therefore,
 obliquity transitioned from a secondary modulator of *G. ruber* white Mg/Ca-based SST during the early Late Pliocene to
 becoming the primary determinant in the early Pleistocene. These findings underscore ice volume fluctuations as the crucial
 factor driving the pace of orbital-scale climate variability in the mid-latitude North Atlantic.

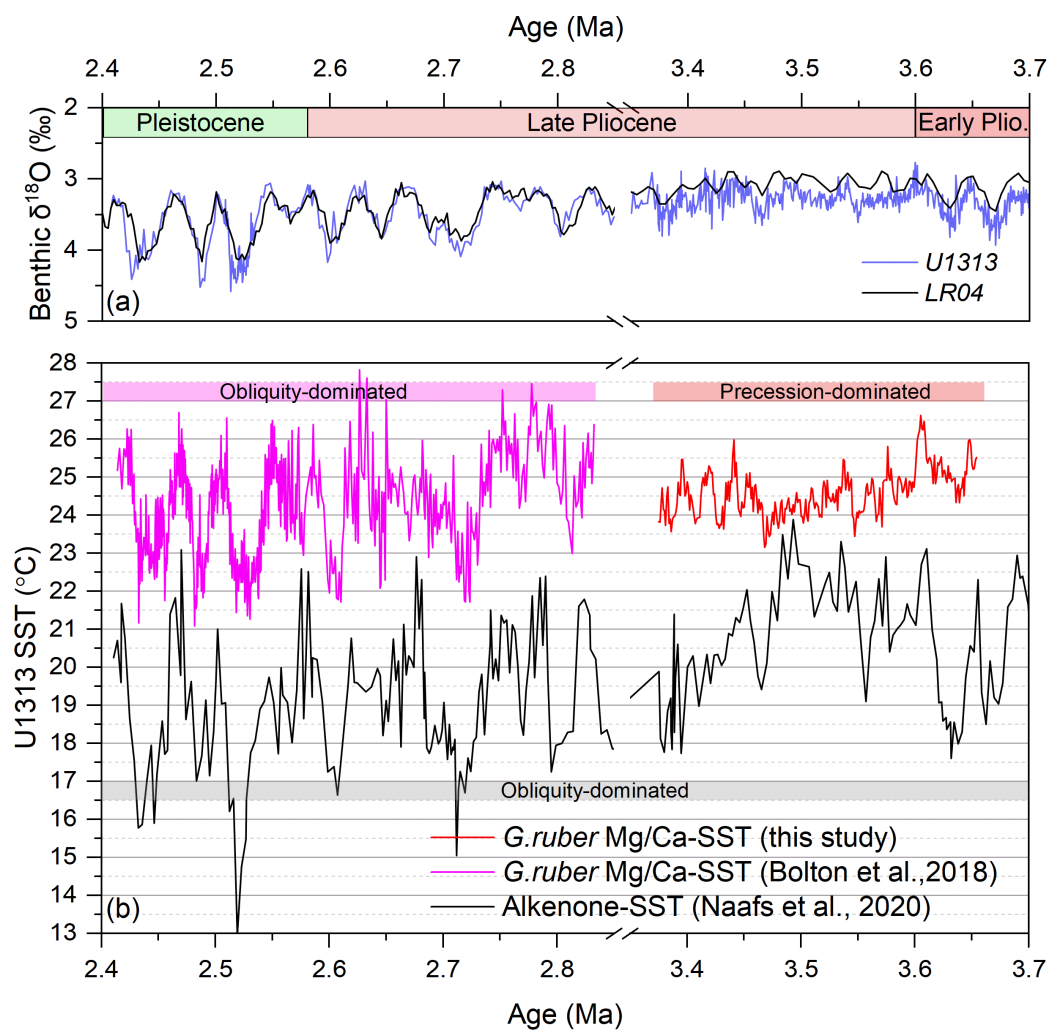


Figure 6. Comparison of the SST records between the Late Pliocene and Early Pleistocene. (a) Benthic $\delta^{18}\text{O}$ of LR04 Stack (Lisiecki and
 385 Raymo, 2005) and Site U1313 (Naafs et al., 2020). (b) *G. ruber* white Mg/Ca-based SST (pink; Bolton et al., 2018; red, this study) and
 alkenone-based SST (black; Naafs et al., 2020)



5. Conclusions

In this study, we present high-resolution *G. ruber* white Mg/Ca-based SST and *G. hirsuta* Mg/Ca-based SubT records from the early Late Pliocene (3.65 – 3.37 Ma), coinciding with the oNHG, at IODP Site U1313 in the mid-latitude North Atlantic. The *G. ruber* white Mg/Ca-based SST, reflecting summer temperatures, were found to be higher by up to 3°C compared to modern summer conditions at the same Site, indicating a consistent northward expansion of the warm STG waters during the early Late Pliocene.

When comparing our new *G. ruber* white Mg/Ca-based SST records with previously published alkenone-based SST records from the same Site, significant differences were noted in both the absolute values and the changing patterns. These discrepancies underscore the distinct seasonal sensitivities of the two proxies, revealing contrasting seasonal SST variations. Our findings suggest that the *G. ruber* white Mg/Ca-based SST are influenced by summer insolation as mirrored in the dominance of the precession cycle, whereas the obliquity dominated alkenone-based SSTs more likely reflect cold season (spring) changes.

A simultaneous long-term decline in both Mg/Ca-based SST and SubT records from 3.65 to 3.5 Ma indicates a reduction in poleward heat transport, pointing to a weakening of the NAC. This observation lends support to the hypothesis that a reduced NAC may have played a role in initiating the Northern Hemisphere Glaciation (Karas et al., 2020).

Moreover, a comparison of the *G. ruber* Mg/Ca-based SST records from the Late Pliocene to the early Pleistocene demonstrates significant shifts in the amplitude of temperature changes and in the dominant climatic cycles. The amplitude of SST variations increased from approximately 2°C in the Late Pliocene to about 4°C in the early Pleistocene, with a marked transition from the precession to the obliquity cycle. This change is attributed to ice-albedo feedback mechanisms and the progressive build-up of ice volume, which together significantly enhanced the influence of obliquity on climate dynamics.

Data Availability. The new data from this paper will be archived at PANGAEA and released after publication of the manuscript.

Author contributions. XP and AV initiated and designed the study. XP generated and analyzed Mg/Ca data with laboratory support from SL. XP prepared the manuscript with contributions from all co-authors.

Competing interests. The authors declare that they have no conflict of interest.

Acknowledgements. This research used samples provided by the Integrated Ocean Drilling Program (IODP). We greatly thank the Bremen Core Repository personnel for collecting the samples (request 20250B of AV) and the student helpers/technicians in the Marine Geology department who washed the samples. We thank Liping Zhou for his insightful comments and facilitating laboratory support. AV received Portuguese national funds from FCT - Foundation for Science and Technology through projects UIDB/04326/2020 (DOI:10.54499/UIDB/04326/2020), UIDP/04326/2020 (DOI:10.54499/UIDP/04326/2020) and LA/P/0101/2020 (DOI:10.54499/LA/P/0101/2020).



References

- 420 Anand, P., Elderfield, H., and Conte, M. H.: Calibration of Mg/Ca thermometry in planktonic foraminifera from a sediment trap time series, *Paleoceanography*, 18, n/a-n/a, <https://doi.org/10.1029/2002pa000846>, 2003.
- Bahr, A., Jaeschke, A., Hou, A., Meier, K., Chiessi, C. M., Albuquerque, A. L. S., Rethemeyer, J., and Friedrich, O.: A Comparison Study of Mg/Ca-, Alkenone-, and TEX86-Derived Temperatures for the Brazilian Margin, *Paleoceanogr. Paleoclimatology*, 38, <https://doi.org/10.1029/2023pa004618>, 2023.
- 425 Bailey, I., Hole, G. M., Foster, G. L., Wilson, P. A., Storey, C. D., Trueman, C. N., and Raymo, M. E.: An alternative suggestion for the Pliocene onset of major northern hemisphere glaciation based on the geochemical provenance of North Atlantic Ocean ice-rafted debris, *Quaternary Sci Rev*, 75, 181–194, <https://doi.org/10.1016/j.quascirev.2013.06.004>, 2013.
- Barker, S., Greaves, M., and Elderfield, H.: A study of cleaning procedures used for foraminiferal Mg/Ca paleothermometry, *Geochem Geophys Geosystems*, 4, n/a-n/a, <https://doi.org/10.1029/2003gc000559>, 2003.
- 430 Bolton, C. T., Bailey, I., Friedrich, O., Tachikawa, K., Garidel-Thoron, T., Vidal, L., Sonzogni, C., Marino, G., Rohling, E. J., Robinson, M. M., Ermini, M., Koch, M., Cooper, M. J., and Wilson, P. A.: North Atlantic Midlatitude Surface-Circulation Changes Through the Plio-Pleistocene Intensification of Northern Hemisphere Glaciation, *Paleoceanogr Paleoclimatology*, 33, 1186–1205, <https://doi.org/10.1029/2018pa003412>, 2018.
- 435 Bridges, J. D., Tarduno, J. A., Cottrell, R. D., and Herbert, T. D.: Rapid strengthening of westerlies accompanied intensification of Northern Hemisphere glaciation, *Nat. Commun.*, 14, 3905, <https://doi.org/10.1038/s41467-023-39557-4>, 2023.
- Carton, J. A. and Giese, B. S.: A Reanalysis of Ocean Climate Using Simple Ocean Data Assimilation (SODA), *Mon. Weather Rev.*, 136, 2999–3017, <https://doi.org/10.1175/2007mwr1978.1>, 2008.
- 440 Catunda, M. C. A., Bahr, A., Kaboth-Bahr, S., Zhang, X., Foukal, N. P., and Friedrich, O.: Subsurface Heat Channel Drove Sea Surface Warming in the High-Latitude North Atlantic During the Mid-Pleistocene Transition, *Geophys Res Lett*, 48, <https://doi.org/10.1029/2020gl091899>, 2021.
- Cavaleiro, C., Voelker, A. H. L., Stoll, H., Baumann, K.-H., Kulhanek, D. K., Naafs, B. D. A., Stein, R., Grützner, J., Ventura, C., and Kucera, M.: Insolation forcing of coccolithophore productivity in the North Atlantic during the Middle Pleistocene, *Quat. Sci. Rev.*, 191, 318–336, <https://doi.org/10.1016/j.quascirev.2018.05.027>, 2018.
- 445 Cléroux, C., Cortijo, E., Anand, P., Labeyrie, L., Bassinot, F., Caillon, N., and Duplessy, J.: Mg/Ca and Sr/Ca ratios in planktonic foraminifera: Proxies for upper water column temperature reconstruction, *Paleoceanography*, 23, n/a-n/a, <https://doi.org/10.1029/2007pa001505>, 2008.
- Cléroux, C., deMenocal, P., Arbuszewski, J., and Linsley, B.: Reconstructing the upper water column thermal structure in the Atlantic Ocean, *Paleoceanography*, 28, 503–516, <https://doi.org/10.1002/palo.20050>, 2013.
- 450 Clotten, C., Stein, R., Fahl, K., and Schepper, S. D.: Seasonal sea ice cover during the warm Pliocene: Evidence from the Iceland Sea (ODP Site 907), *Earth Planet. Sci. Lett.*, 481, 61–72, <https://doi.org/10.1016/j.epsl.2017.10.011>, 2018.
- de la Vega, E., Chalk, T. B., Wilson, P. A., Bysani, R. P., and Foster, G. L.: Atmospheric CO₂ during the Mid-Piacenzian Warm Period and the M2 glaciation, *Sci Rep-uk*, 10, 11002, <https://doi.org/10.1038/s41598-020-67154-8>, 2020.
- 455 De Schepper, S., Head, M. J., and Groeneveld, J.: North Atlantic Current variability through marine isotope stage M2 (circa 3.3 Ma) during the mid-Pliocene, *Paleoceanography*, 24, <https://doi.org/10.1029/2008pa001725>, 2009.
- Dowsett, H., Dolan, A., Rowley, D., Pound, M., Salzmann, U., Robinson, M., Chandler, M., Foley, K., and Haywood, A.: The PRISM4 (mid-Piacenzian) palaeoenvironmental reconstruction, *Clim Past Discuss*, 0, 1–39, <https://doi.org/10.5194/cp-2016-33>, 2016.
- 460 Dowsett, H. J., Robinson, M. M., Haywood, A. M., Hill, D. J., Dolan, A. M., Stoll, D. K., Chan, W.-L., Abe-Ouchi, A., Chandler, M. A., Rosenbloom, N. A., Otto-Bliesner, B. L., Bragg, F. J., Lunt, D. J., Foley, K. M., and Riesselman, C. R.: Assessing confidence in Pliocene sea surface temperatures to evaluate predictive models, *Nat Clim Change*, 2, 365–371, <https://doi.org/10.1038/nclimate1455>, 2012.
- Expedition 306 Scientists: Proceedings of the IODP, 303/306, Proc. IODP, <https://doi.org/10.2204/iodp.proc.303306.112.2006>, 2006.
- 465 Evans, D. and Müller, W.: Deep time foraminifera Mg/Ca paleothermometry: Nonlinear correction for secular change in seawater Mg/Ca, *Paleoceanography*, 27, <https://doi.org/10.1029/2012pa002315>, 2012.



- Fan, Y., Liu, W., Zhang, P., Chen, R., and Li, L.: North Atlantic Oscillation contributes to the subpolar North Atlantic cooling in the past century, *Clim. Dyn.*, 61, 5199–5215, <https://doi.org/10.1007/s00382-023-06847-y>, 2023.
- 470 Fedorov, A. V., Brierley, C. M., Lawrence, K. T., Liu, Z., Dekens, P. S., and Ravelo, A. C.: Patterns and mechanisms of early Pliocene warmth, *Nature*, 496, 43–49, <https://doi.org/10.1038/nature12003>, 2013.
- Friedrich, O., Schiebel, R., Wilson, P. A., Weldeab, S., Beer, C. J., Cooper, M. J., and Fiebig, J.: Influence of test size, water depth, and ecology on Mg/Ca, Sr/Ca, $\delta^{18}\text{O}$ and $\delta^{13}\text{C}$ in nine modern species of planktic foraminifers, *Earth Planet Sc Lett*, 319, 133–145, <https://doi.org/10.1016/j.epsl.2011.12.002>, 2012.
- 475 Friedrich, O., Wilson, P. A., Bolton, C. T., Beer, C. J., and Schiebel, R.: Late Pliocene to early Pleistocene changes in the North Atlantic Current and suborbital-scale sea-surface temperature variability, *Paleoceanography*, 28, 274–282, <https://doi.org/10.1002/palo.20029>, 2013.
- Hammer, Ø. and Harper, D. A.: Past: paleontological statistics software package for education and data analysis, *Palaeontologia electronica*, 4, 1, http://palaeo-electronica.org/2001_1/past/issue1_01.htm, 2001.
- 480 Haywood, A. M., Dowsett, H. J., and Dolan, A. M.: Integrating geological archives and climate models for the mid-Pliocene warm period, *Nat Commun*, 7, 10646, <https://doi.org/10.1038/ncomms10646>, 2016.
- Hennissen, J. A. I., Head, M. J., Schepper, S. D., and Groeneveld, J.: Palynological evidence for a southward shift of the North Atlantic Current at ~2.6 Ma during the intensification of late Cenozoic Northern Hemisphere glaciation, *Paleoceanography*, 29, 564–580, <https://doi.org/10.1002/2013pa002543>, 2014.
- 485 Hennissen, J. A. I., Head, M. J., Schepper, S. D., and Groeneveld, J.: Increased seasonality during the intensification of Northern Hemisphere glaciation at the Pliocene–Pleistocene boundary ~2.6 Ma, *Quat. Sci. Rev.*, 129, 321–332, <https://doi.org/10.1016/j.quascirev.2015.10.010>, 2015.
- Karas, C., Khélifi, N., Bahr, A., Naafs, B. D. A., Nürnberg, D., and Herrle, J. O.: Did North Atlantic cooling and freshening from 3.65–3.5 Ma precondition Northern Hemisphere ice sheet growth?, *Global Planet Change*, 185, 103085, <https://doi.org/10.1016/j.gloplacha.2019.103085>, 2020.
- 490 Knies, J., Cabedo-Sanz, P., Belt, S. T., Baranwal, S., Fietz, S., and Rosell-Melé, A.: The emergence of modern sea ice cover in the Arctic Ocean, *Nat. Commun.*, 5, 5608, <https://doi.org/10.1038/ncomms6608>, 2014.
- Laskar, J., Robutel, P., Joutel, F., Gastineau, M., Correia, A. C. M., and Levrard, B.: A long-term numerical solution for the insolation quantities of the Earth, *Astron. Astrophys.*, 428, 261–285, <https://doi.org/10.1051/0004-6361:20041335>, 2004.
- 495 Lawrence, K. T. and Woodard, S. C.: Past sea surface temperatures as measured by different proxies—A cautionary tale from the late Pliocene, *Paleoceanography*, 32, 318–324, <https://doi.org/10.1002/2017pa003101>, 2017.
- Lawrence, K. T., Herbert, T. D., Brown, C. M., Raymo, M. E., and Haywood, A. M.: High-amplitude variations in North Atlantic sea surface temperature during the early Pliocene warm period, *Paleoceanography*, 24, n/a-n/a, <https://doi.org/10.1029/2008pa001669>, 2009.
- 500 Lawrence, K. T., Sosdian, S., White, H. E., and Rosenthal, Y.: North Atlantic climate evolution through the Plio-Pleistocene climate transitions, *Earth Planet Sc Lett*, 300, 329–342, <https://doi.org/10.1016/j.epsl.2010.10.013>, 2010.
- Leduc, G., Schneider, R., Kim, J.-H., and Lohmann, G.: Holocene and Eemian sea surface temperature trends as revealed by alkenone and Mg/Ca paleothermometry, *Quaternary Sci Rev*, 29, 989–1004, <https://doi.org/10.1016/j.quascirev.2010.01.004>, 2010.
- 505 Lee, K. E., Clemens, S. C., Kubota, Y., Timmermann, A., Holbourn, A., Yeh, S.-W., Bae, S. W., and Ko, T. W.: Roles of insolation forcing and CO₂ forcing on Late Pleistocene seasonal sea surface temperatures, *Nat. Commun.*, 12, 5742, <https://doi.org/10.1038/s41467-021-26051-y>, 2021.
- Lévy, M., Lehahn, Y., André, J., Mémerly, L., Loisel, H., and Heifetz, E.: Production regimes in the northeast Atlantic: A study based on Sea-viewing Wide Field-of-view Sensor (SeaWiFS) chlorophyll and ocean general circulation model mixed layer depth, *J. Geophys. Res.: Oceans*, 110, <https://doi.org/10.1029/2004jc002771>, 2005.
- 510 Lisiecki, L. E. and Raymo, M. E.: A Pliocene-Pleistocene stack of 57 globally distributed benthic $\delta^{18}\text{O}$ records: PLIOCENE-PLEISTOCENE BENTHIC STACK, *Paleoceanography*, 20, n/a-n/a, <https://doi.org/10.1029/2004pa001071>, 2005.
- 515 Locarnini, R. A., Mishonov, A. V., Antonov, J. I., Boyer, T. P., Garcia, H. E., Baranova, O. K., Zweng, M. M., Paver, C. R., Reagan, J. R., Johnson, D. R., Hamilton, M., Danabasoglu, K., Seidov, and Levitus, S.: World ocean atlas 2013. Volume 1, Temperature, <https://doi.org/10.7289/v55x26vd>, 2013.



- 520 McClymont, E. L., Ho, S. L., Ford, H. L., Bailey, I., Berke, M. A., Bolton, C. T., Schepper, S., Grant, G. R., Groeneveld, J.,
Inglis, G. N., Karas, C., Patterson, M. O., Swann, G. E. A., Thirumalai, K., White, S. M., Alonso-Garcia, M.,
Anand, P., Hoogakker, B. A. A., Littler, K., Petrick, B. F., Risebrobakken, B., Abell, J. T., Crocker, A. J., Graaf, F.,
Feakins, S. J., Hargreaves, J. C., Jones, C. L., Markowska, M., Ratnayake, A. S., Stepanek, C., and Tanguan, D.:
Climate Evolution Through the Onset and Intensification of Northern Hemisphere Glaciation, *Rev. Geophys.*, 61,
<https://doi.org/10.1029/2022rg000793>, 2023.
- 525 Meyers, S. R. and Hinnov, L. A.: Northern Hemisphere glaciation and the evolution of Plio-Pleistocene climate noise,
Paleoceanography, 25, <https://doi.org/10.1029/2009pa001834>, 2010.
- Mudelsee, M. and Raymo, M. E.: Slow dynamics of the Northern Hemisphere glaciation, *Paleoceanography*, 20, n/a-n/a,
<https://doi.org/10.1029/2005pa001153>, 2005.
- Naafs, B. D. A., Stein, R., Hefter, J., Khélifi, N., Schepper, S. D., and Haug, G. H.: Late Pliocene changes in the North
Atlantic Current, *Earth Planet Sc Lett*, 298, 434–442, <https://doi.org/10.1016/j.epsl.2010.08.023>, 2010.
- 530 Naafs, B. D. A., Hefter, J., Acton, G., Haug, G. H., Martínez-García, A., Pancost, R., and Stein, R.: Strengthening of North
American dust sources during the late Pliocene (2.7Ma), *Earth Planet Sc Lett*, 317, 8–19,
<https://doi.org/10.1016/j.epsl.2011.11.026>, 2012.
- Naafs, B. D. A., Voelker, A. H. L., Karas, C., Andersen, N., and Sierro, F. J.: Repeated Near-Collapse of the Pliocene Sea
Surface Temperature Gradient in the North Atlantic, *Paleoceanogr Paleoclimatology*, 35,
535 <https://doi.org/10.1029/2020pa003905>, 2020.
- Paillard, D., Labeyrie, L., and Yiou, P.: Macintosh Program performs time-series analysis, *Eos, Trans. Am. Geophys. Union*,
77, 379–379, <https://doi.org/10.1029/96eo00259>, 1996.
- Rebotim, A., Voelker, A. H. L., Jonkers, L., Waniek, J. J., Schulz, M., and Kucera, M.: Calcification depth of deep-dwelling
planktonic foraminifera from the eastern North Atlantic constrained by stable oxygen isotope ratios of shells from
540 stratified plankton tows, *J Micropalaeontol*, 38, 113–131, <https://doi.org/10.5194/jm-38-113-2019>, 2019.
- Reiðig, S., Nürnberg, D., Bahr, A., Poggemann, D. -W., and Hoffmann, J.: Southward Displacement of the North Atlantic
Subtropical Gyre Circulation System During North Atlantic Cold Spells, *Paleoceanogr Paleoclimatology*, 34, 866–
885, <https://doi.org/10.1029/2018pa003376>, 2019.
- 545 Repschläger, J., Weinelt, M., Schneider, R., Blanz, T., Leduc, G., Schiebel, R., and Haug, G. H.: Disentangling multiproxy
temperature reconstructions from the subtropical North Atlantic, *Front. Ecol. Evol.*, 11, 1176278,
<https://doi.org/10.3389/fevo.2023.1176278>, 2023.
- Robinson, M. M., Dowsett, H. J., Dwyer, G. S., and Lawrence, K. T.: Reevaluation of mid-Pliocene North Atlantic sea
surface temperatures, *Paleoceanography*, 23, n/a-n/a, <https://doi.org/10.1029/2008pa001608>, 2008.
- 550 The Cenozoic CO₂ Proxy Integration Project (CenCO₂PIP) Consortium*†.: Toward a Cenozoic history of atmospheric CO₂,
Science, 382, eadi5177, <https://doi.org/10.1126/science.adi5177>, 2023.
- Westerhold, T., Marwan, N., Drury, A. J., Liebrand, D., Agnini, C., Anagnostou, E., Barnet, J. S. K., Bohaty, S. M.,
Vleeschouwer, D. D., Florindo, F., Frederichs, T., Hodell, D. A., Holbourn, A. E., Kroon, D., Lauretano, V., Littler,
K., Lourens, L. J., Lyle, M., Pälike, H., Röhl, U., Tian, J., Wilkens, R. H., Wilson, P. A., and Zachos, J. C.: An
astronomically dated record of Earth’s climate and its predictability over the last 66 million years, *Science*, 369,
555 1383–1387, <https://doi.org/10.1126/science.aba6853>, 2020.
- Zhou, X., Rosenthal, Y., Haynes, L., Si, W., Evans, D., Huang, K.-F., Hönisch, B., and Erez, J.: Planktic foraminiferal
Na/Ca: A potential proxy for seawater calcium concentration, *Geochim Cosmochim Acta*, 305, 306–322,
<https://doi.org/10.1016/j.gca.2021.04.012>, 2021.